diversity

MDPI

Article

Characterization and Comparison of Eye Development and Phototransduction Genes in Deep- and Shallow-Water Shrimp *Alvinocaris longirostris* and *Palaemon carinicauda*

Min Hui [1,2,3,*], Qian Xin [1,2,3], Jiao Cheng [1,2,3] and Zhongli Sha [1,2,3,*]

[1] Department of Marine Organism Taxonomy & Phylogeny, Institute of Oceanology, Chinese Academy of Sciences, Qingdao 266071, China
[2] Laboratory for Marine Biology and Biotechnology, Qingdao National Laboratory for Marine Science and Technology, Qingdao 266237, China
[3] Shandong Province Key Laboratory of Experimental Marine Biology, Institute of Oceanology, Chinese Academy of Sciences, Qingdao 266071, China
* Correspondence: minhui@qdio.ac.cn (M.H.); shazl@qdio.ac.cn (Z.S.)

Abstract: The investigations of the molecular components of eye development and phototransduction in deep-sea species are important to elucidate the mechanism of their adaptation to dim light. In this study, eye transcriptomes of the shrimp *Alvinocaris longirostris* from the deep-sea chemosynthetic ecosystem and the shallow-water shrimp *Palaemon carinicauda* were compared. Two *Pax6* homologs with low expression levels were identified in both species, which are essential transcription factors in eye development. This finding implies that the development of the two shrimp eyes at early embryo–larvae stages might be similar. The multiple components of the phototransduction pathway were identified in both species. However, the number of phototransduction components was significantly reduced in *A. longirostris*, as well as expression level. Particularly, short-wavelength/UV-sensitive (SWS/UVS) *opsins* were absent in *A. longirostris* and only one putative middle-wavelength-sensitive (MWS) *opsin* was identified in this species. The conserved sites and structures of the putative LWS opsins were found between deep-sea and shallow-water decapods, indicating that the opsins in deep-sea crustaceans may also conserve their spectral absorption and signal transduction function. Phylogenetic analyses supported the monophyly of LWS opsins and SWS/UVS opsins in arthropods, while the MWS clade fell outside of the main arthropod LWS clade. The results are expected to provide baseline for study of visual adaptation in deep-sea shrimps.

Keywords: alvinocarididae; deep sea; opsin; pax 6; phototransduction; transcriptome

Citation: Hui, M.; Xin, Q.; Cheng, J.; Sha, Z. Characterization and Comparison of Eye Development and Phototransduction Genes in Deep- and Shallow-Water Shrimp *Alvinocaris longirostris* and *Palaemon carinicauda*. *Diversity* **2022**, *14*, 653. https://doi.org/10.3390/d14080653

Academic Editor: Michael Wink

Received: 16 June 2022
Accepted: 8 August 2022
Published: 12 August 2022

1. Introduction

Deep-sea hydrothermal vents and cold seeps are unique ecosystems with extreme properties, such as dim light, high pressure and chemical rich waters, which present exceptional challenges to organisms [1,2]. No sunlight penetrates these deep-sea (below 1000 m) chemosynthetic environments, and the ambient light is usually composed of bioluminescence and chemiluminescence [3–6]. These special conditions have a profound effect on the designs of animal eyes optically and neurally [7].

The eyes of crustaceans from the deep sea have developed various characteristics. Many species have small or degenerate eyes with reduced ommatidia (e.g., euphausiid *Thysanopoda minyops*, *Bentheuphausia amblyops* and shrimp *Alvinocaris markensis*) [8–10]. In contrast, some other crustaceans are equipped with large eyes and have enlarged corneal facets and massive rhabdoms in order to maximize the sensitivity to dim light (e.g., crab *Paralomis multispina*, isopod *Bathynomus giganteus* and mysid *Boreomysis scyphops*) [11–13]. Moreover, a 'dorsal eye' has formed in the hydrothermal vent blind shrimp *Rimicaris exoculata*, lacking an externally differentiated eye [14], and the adult vent crab *Bythograea thermydron*

possesses 'naked retina' eyes which lose their image-forming optics and develop high photon sensitivity [15]. However, the molecular mechanisms illustrating the eye development and function in deep sea crustaceans remain uncovered due to the difficulties in deep-sea study, especially in the culture of deep-sea animals.

The previous studies of tissue-specific transcription factors have improved our understanding of retinal determination networks that influence eye development in invertebrates (Figure S1; revised according to [16]), including two major transcription factors, *eyeless* (*ey*) and *twin of eyeless* (*toy*) (both paired-homeodomain *Pax6* homologs). The mutations or misexpression of the two upstream regulatory genes can lead to defects of eye development or ectopic eye in *Drosophila* [17]. A series of genes encoding transcription factors act downstream, including *sine oculis* (*so*), *eyes absent* (*eya*), *dachshund* (*dac*), *hedgehog* (*hh*) and *decapentaplegic* (*dpp*) (Figure S1). They regulate each other to determine eye development [18–20]. It has been found that the knockdown of *dac* causes strong but incomplete adult eye reduction in flies [21]. One of the most extensive investigations of the eye degeneration of aquatic animals focused on cavefish and their conspecific or closely related surface-dwelling species, showing that the reduced transcription of phototransduction-related genes and the down- or over-expression of different transcriptional factors have direct roles in the retinal development, maintenance and function of cavefish [22–24]. Increasing studies have also shown that variation in gene regulation, rather than mutational differences, is largely responsible for phenotypic variance among closely related organisms [25]. Therefore, retinal degeneration can occur by different developmental molecular mechanisms.

The phototransduction signaling cascade in invertebrates is usually initiated by the light-activation of rhodopsin that stimulates the G-protein and phospholipase C (PLC), leading to the opening of the cation-selective transient receptor potential (TRP) channels, and transient receptor potential-like (TRPL) channels [26]. The most commonly studied components of phototransduction pathway are the photoreceptor opsins [27], which have been divided into three groups based on the maximal absorbance (λ_{max}), long-wavelength-sensitive (LWS), middle-wavelength-sensitive (MWS), and short-wavelength/UV-sensitive (SWS/UVS) opsins. In the study by Porter et al. [28], SWS/UVS visual pigments were defined as those with λ_{max} ranging from 300 to 400 nm, MWS pigments as those with 400–490 nm and LWS pigments as those with greater than 490 nm. Photoreceptor opsins in crustacean eyes are diverse. A single crustacean species may include only one spectral photoreceptor class or dozens of different spectral receptor types, which is partly explained by the various habitat types occupied by crustaceans, from deep sea to intertidal and even terrestrial niches [29]. Studies between cave and surface crustaceans or fish have detected mutations and the down-regulation of visual-related genes in dark cave species [30–34]. A reduction in the total absorbance spectra of eye photoreceptor visual pigments was also discovered in the cave species compared to the epigeal species [35].

The caridean shrimp genus *Alvinocaris* (Crustacea: Caridea: Alvinocarididae) is known from chemosynthetic communities associated with deep-sea hydrothermal vents or cold seeps. Morphologically, all the species in this genus retain the regressive eye structure, lacking corneal facets, but usually with diffused pigmentation inside [36]. The examination of the structure and ultrastructure of a species in genus *Alvinocaris* has found that the expected massive array of photoreceptors is partially missing, showing a regressive eye structure [10]. Therefore, the shrimps of genus *Alvinocaris* presents an operable object to study the molecular mechanisms of eye degeneration and the visual adaptation of shrimps inhabiting deep-sea chemosynthetic ecosystems. However, before we can do so, we must firstly elucidate those molecular components related to eye development and phototransduction.

In this study, we characterized and compared the previous reported eye transcriptome of *A. longirostris* showing regressive eye structure and from a deep-sea chemosynthetic ecosystem (Figure 1a,b) and the newly sequenced eye transcriptome of a shallow-sea shrimp *Palaemon carinicauda* (Palaemonidae) with normal compound eyes (Figure 1c), which also

belongs to Caridea and appears relatively closely related with Alvinocarididae in phylogeny [37]. In detail, we performed (1) the identification of key molecular components and the expression of homologous genes from known eye development and phototransduction pathways in the two shrimp species, and (2) the comparison of diversity, expression level and phylogeny of these key genes from deep and shallow-water shrimps to present the primary view of the molecular basis of eye development and vision in shrimps from deep sea chemosynthetic environments and broaden insights into crustaceans' visual systems.

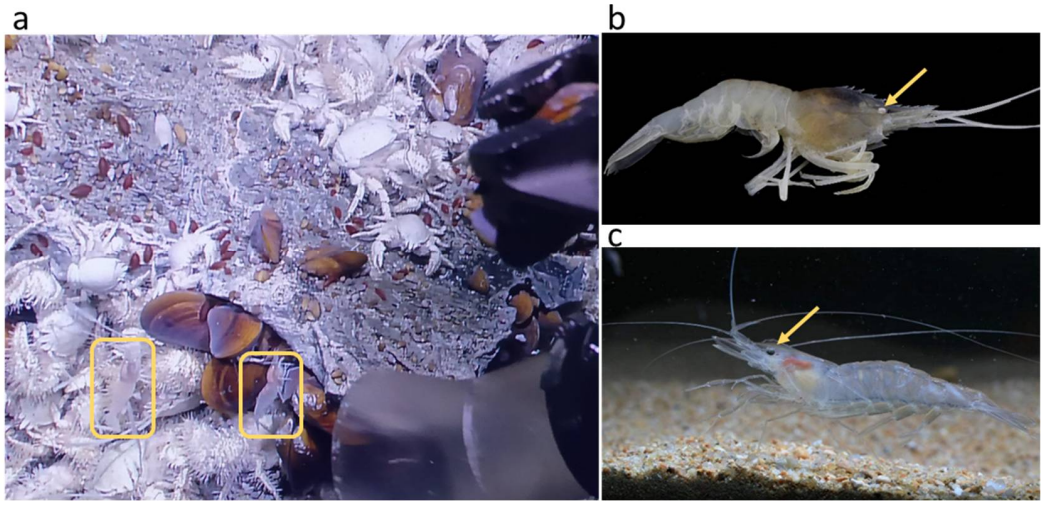

Figure 1. The living environment of deep-sea seep *Alvinocaris longirostris* (**a**), and photos of *A. longirostris* (**b**) and *Palaemon carinicauda* (**c**). The photos (**b**,**c**) are taken by Ziming Yuan and Chengzhang Liu, respectively. Shrimps *A. longirostris* are marked with yellow squares. The eyes of the two shrimp species are identified by the arrows.

2. Materials and Methods

2.1. Sample Collection

The *A. longirostris* (Figure 1a,b) samples were collected near a methane seep in the South China Sea (22°6.9′ N, 119°17.1′ E, depth 1119.2 m) in September 2017. In order to reduce the damage to the retinal tissues of these deep-sea animals caused by the surface light, they were captured at night by the remotely operated vehicle (ROV) Quasar MkII on the scientific research vessel (RV) KEXUE (Institute of Oceanology, Chinese academy of Sciences, China) and placed into the light-tight and insulated Bio-Boxes. After being brought on board, the eyes of *A. longirostris* were dissected under dim light and frozen in liquid nitrogen immediately. The samples had been stored in liquid nitrogen until returning to the lab. The sampling method and transcriptome sequencing data for the eyes of six *A. longirostris* individuals were described in our previous study [38]. Shallow-water *P. carinicauda* (Figure 1c) samples were acquired from the aquarium in the Institute of Oceanology, Chinese Academy of Sciences. After taken, the eye tissues of the species were dissected and immediately frozen in liquid nitrogen for RNA extraction.

2.2. Transcriptome Sequencing and Assembly

Total RNA for three samples of *P. carinicauda* eyes was extracted using the TRIzol kit (Invitrogen, Waltham, MA, USA), respectively, and was mixed equally. After treatment, the fragmented mRNAs were used to construct the cDNA libraries with NEBNext® Ultra™ RNA Library as our previous study [38]. Then the library was sequenced on an Illumina HiSeq™ 4000 platform following the manufacturer's instructions (Illumina, San Diego, SA, USA) and paired-end reads with length 150 bp were produced. To obtain clean reads, the raw reads were filtered by removing reads containing an adaptor, ploy-*N* (with the ratio of '*N*' > 10%) and low quality reads (percentage of bases with Q value < 20 in the sequence was >40%) through custom perl scripts. Here, Q value was a quality index to

assess reliability of a base calling, and a higher Q value presented a more reliable base calling. Transcriptome de novo assembly was carried out by using Trinity v2.2.1 [39] with default parameters, except min_kmer_cov set to four in order to reduce the redundancy of the assembled transcripts. The modules of Inchworm, Chrysalis and Butterfly in Trinity were then used to assemble the clean sequences into contigs, de Bruijin graphs and full-length transcripts sequentially. The one with the longest length of redundant transcripts was defined as a unigene. The average length and N50 length of unigenes were calculated through home-made perl scripts. All unigenes were arranged in length descending order, and when the assembled length covered half of the total length of all unigenes, the length of the current unigenes was considered to be N50. The completeness and redundancy of the assembled transcriptome was evaluated by checking the coverage of the 1066 conserved core genes of arthropoda (https://busco.ezlab.org/, accessed on 18 July 2022) with BUSCO v5.3.2 [40,41].

2.3. Gene Functional Annotation and Expression Analysis

Functional annotations for the unigenes were carried out through BLAST against the NR (NCBI non-redundant protein sequences), Swiss-Prot (http://www.ebi.ac.uk/uniprot/; accessed on 3 August 2021), KEGG (Kyoto Encyclopedia of Genes and Genomes, https://www.kegg.jp/kegg/; accessed on 4 August 2021) and KOG (euKaryotic Ortholog Group, http://www.ncbi.nlm.nih.gov/COG/; accessed on 4 August 2021) databases with an E-value $\leq$ 1E-5. GO (Gene Ontology) annotation was obtained using software blast2GO [42] based on NR annotation results with a cut-off E-value threshold 1E-5. All unigenes with GO annotations were functionally classified using software WEGO [43]. Gene expression levels were estimated by RPKM (Reads Per kb per Million reads) method [44].

2.4. Phylogenetic and Evolutionary Analyses

In order to investigate the diversity and evolutionary positions of the key phototransduction components, opsins in *A. longirostris* and *P. carinicauda* were identified from the transcriptomes according to the unigene annotation and further manual check by blast analysis. The phylogenetic tree was constructed for 127 opsin sequences of representative arthropod species (Table S1). In detail, the dataset comprised five opsins from *A. longirostris*, 13 opsins from *P. carinicauda* and 109 opsins with different wavelength sensitivity (65 LWS, 19 MWS and 25 SWS opsins) from other arthropods downloaded from NCBI or obtained by personal communication. Among them, opsins from three other deep-sea shrimps, *Janicella spinicauda*, *Systellaspis debilis* and *Oplophorus gracilirostris*, belonging to Oplophoridae were also included, which have compound eyes and light organs (photophores) [45,46]. *Bos taurus* rhodopsin and *Gallus gallus* pinopsin sequences served as out-group. Amino acid sequences were aligned using MAFFT (https://mafft.cbrc.jp/alignment/server/, accessed on 14 July 2022) [47,48] and the resulting alignment was used to construct a phylogenetic tree with the maximum likelihood (ML) method implemented by IQ-TREE web server (http://iqtree.cibiv.univie.ac.at/, accessed on 14 July 2022) [49]. The substitution model test was run first by the ModelFineder [50] in IQ-TREE. The model LG + R6 + F (a general amino acid replacement matrix, FreeRate model with six rating categories, and empirical base frequencies) was selected. Branch support was assessed in triplicate by (1) a Shimodaira–Hasegawa-like approximate likelihood ratio test (SH-aLRT; 1000 replicates), (2) an approximate Bayes test and (3) an ultra-fast bootstrap approximation (UFBoot; 1000replicates) [51–53]. Images were created using the FigTree 1.4.4 (http://tree.bio.ed.ac.uk/software/figtree/, accessed on 14 July 2022). Similarly, a total of two Pax6 amino acid sequences of *A. longirostris*, two Pax6 of *P. carinicauda* and twelve Pax6 sequences (defined clearly as toy or eye) ofsix other arthropods available in NCBI or obtained by personal communication were used to construct phylogenetic tree with *A. longirostris* Pax2, *J. spinicauda* Pax5 and *Neocaridina davidina* Pax5 as out groups (Table S2). ModelFinder suggested a VT + F + G4 (a general matrix VT model, empirical amino acid frequencies and a discrete gamma model with four rating categories) model.

2.5. Opsin Characterization Analysis

For *opsin* candidates, the open reading frames (ORFs) of the genes were predicted using the ORF Finder (http://www.ncbi.nlm.nih.gov/projects/gorf/, accessed on 4 October 2021). A multiple alignment of 23 opsin amino acid sequences from 14 decapod species including deep-sea and shallow-water species (Table S1) was performed using BioEdit v7.1.3. Sequence alignment made it possible to identify characteristics of opsin sequences, such as the lysine residue involved in the Schiff base linkage, the counterion and putative disulfide bond sites.

3. Results

3.1. Transcriptome Assembly and Functional Annotation

In total, 52,400,160 raw reads of the *P. carinicauda* eye sample were newly obtained and deposited into the Sequence Read Archive (SRA) database (http://www.ncbi.nlm.nih.gov/Traces/sra/; accessed on 22 March 2020) with the accession number PRJNA597836. Removing adaptors and low-quality reads resulted in the retention of 7.62 G clean bases for *P. carinicauda*. Assembly generated 46,709 unigenes for *P. carinicauda*, with the unigene N50 length of 1217 bp. The raw reads of six *A. longirostris* eye samples were available with the accession number PRJNA548620. The number of unigenes of *A. longirostris* eyes was 64,352 and the N50 length was 1868 bp reported in our previous study [36]. BUSCO evaluation identified 788 (73.92%) complete BUSCOs in *P. carinicauda* eye transcriptome, which was lower than that of *A. longirostris* (1009 complete BUSCOs, 94.65%).

Based on the four databases, 16,951 (36.29%) unigenes of *P. carinicauda* were finally annotated in at least one database (Table 1), while 21,922 (34.07%) unigenes of *A. longirostris* were annotated [38]. In KOG cluster, unigenes were classified into 25 functional categories, and 'signal transduction mechanisms' made up a large proportion in the *P. carinicauda* eye transcriptome, as well as in *A. longirostris* eye transcriptome (Figure 2). By KEGG analysis, 8674 (18.57%) unigenes of *P. carinicauda* were found to be involved in 214 different biological pathways, and the largest number of unigenes was assigned to the 'metabolic pathways'. There were 2216 (13.14%) NR-annotated unigenes grouping into 49 subcategories in GO analysis *P. carinicauda* (Figure S2). These gene annotation and classification would facilitate the following interpretation for key genes related to the eye development and phototransduction of the deep-sea and shallow-water shrimps.

Table 1. Summary statistics of transcriptome data from *Palaemon carinicauda* eyes.

Index	Value (Percentage)
Numbers of unigenes	46,709
N50 length of unigenes	1217
Average length of unigenes (bp)	718
Annotated in NR	16,866 (36.11%)
Annotated in Swiss-Prot	12,431 (26.61%)
Annotated in KOG	11,561 (24.75%)
Annotated in KEGG	8674 (18.57%)
Annotated in GO	2216 (13.14%)
Annotated in at least one database	16,951 (36.29%)

3.2. Eye Development Related Genes

To identify genes potentially related to the differences in retinal development and maintenance between adult *A. longirostris* and *P. carinicauda*, seven key transcription factor genes were queried, including *ey*, *toy*, *so*, *eya*, *dac*, *hh* and *dpp*. Among them, *ey* and *toy* were the homologues of *Pax6* in vertebrates. The number of these transcription factor genes was similar in the two species, and the overall expression was relatively low in both species (RPKM value 0.251–4.323, except *eya* in *P. carinicauda* with RPKM 10.163; Table S3). Additionally, two kinds of *Pax6* genes were separately annotated in *A. longirostris* and *P. carinicauda* transcriptomes, including *Al-Pax6.1*, *Al-Pax6.2*, *Pc-Pax6.1* and *Pc-Pax6.2*.

High amino acid sequences sequence similarity (97%) was found between *Al-Pax6.1* and *Pc-Pax6.1*, as well as between *Al-Pax6.2* and *Pc-Pax6.2*. Phylogenetic analysis based on the amino acid sequences of *Pax6* homologues in 16 arthropods (Table S2) showed that *ey* and *toy* were two paralogs [54], and *Al-Pax6.1* and *Al-Pax6.2* were closely related to ey and toy, respectively (Figure 3).

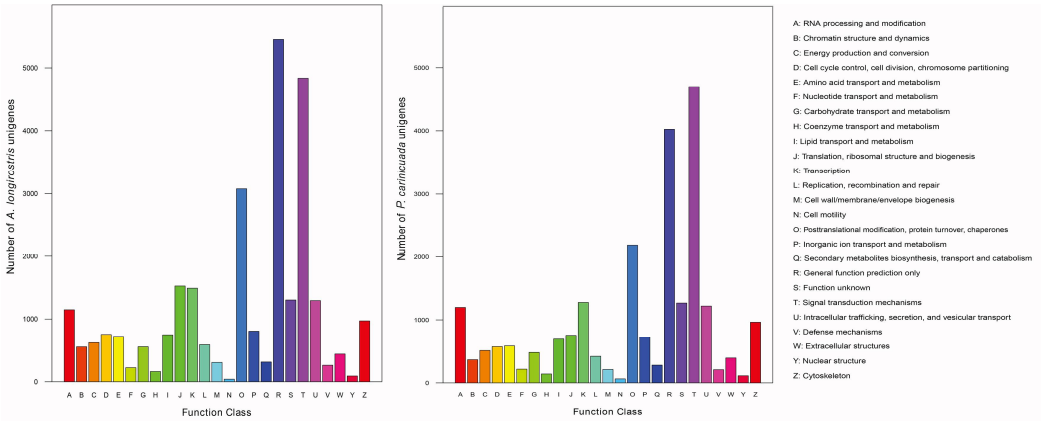

Figure 2. The KOG distribution of annotated genes in the eye transcriptomes of *Alvinocaris longirostris* and *Palaemon carinicauda*.

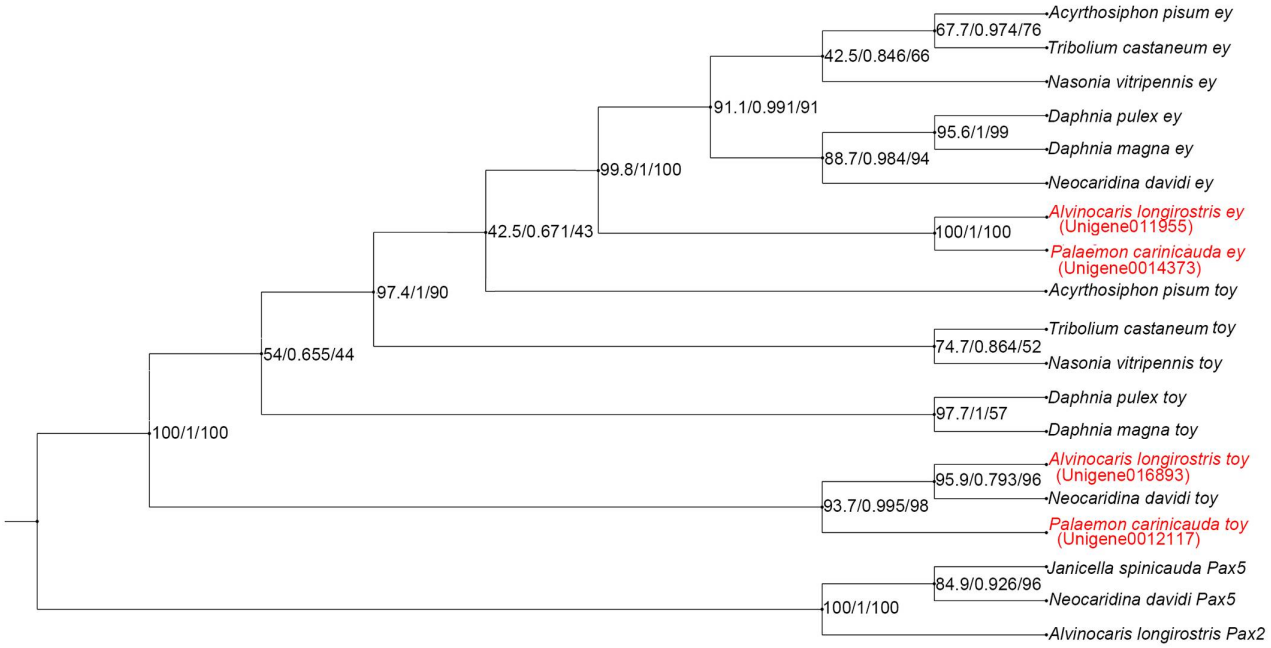

Figure 3. Phylogenetic tree of Pax homologs. Numbers above branches represent branch support values of SH-aLRT support (%)/aBayes support/ultrafast bootstrap support (%).

3.3. Genes Involved in the Phototransduction Pathway

Multiple components of the phototransduction pathway were identified in both species, including opsin, Gq protein, PLC, protein kinase C (PKC), TRP channels, TRPL channels, calmodulin (CaM), neither inactivation nor afterpotential protein C (NINAC), arrestin, diacylglycerol lipase (DAGL), actin and INAD PDZ domains (Table 2). Fewer phototansduction transcripts were found in the deep-sea *A. longirostris* compared to the shallow-water *P. carinicauda* (Figure 4). The most dramatic difference was the number of *opsin* genes (five in *A. longirostris* and thirteen in *P. carinicauda*). According to the RPKM values, the expression of *opsins* in *A. longirostris* (RPKM: 1.53–40.68) was roughly estimated

to be lower than that in *P. carinicauda* (RPKM: 5.03–90,886.59) (Table 2). Specifically, the gene *DAGL* was only found expressed in the adult eye transcriptome of *A. longirostris*. However, an absence of expression does not mean that the genes are not present, considering that the RNAseq data are dependent on the gene expression at time of sampling.

Table 2. Genes involved in the Gq-mediated phototransduction cascade from *Alvinocaris longirostris* and *Palaemon carinicauda*. They include opsin, G-protein, G-protein subunit alpha (Gα), beta (Gβ) and gamma (Gγ), Gq subclass of the G-protein alpha (Gαq) subunits, phospholipase C (PLC), protein kinase C (PKC), transient receptor potential (TRP) channels, transient receptor potential-like (TRPL) channels, calmodulin (CaM), neither inactivation nor afterpotential protein C (NINAC), arrestin, diacylglycerol lipase (DAGL), actin and INAD PDZ domains. RPKM (reads per kb per million reads) shows the gene expression level revealed by RNA-seq.

	Alvinocaris longirostris		***Palaemon carinicauda***		
Gene ID	**RPKM**	**Annotation**	**GeneID**	**RPKM**	**Annotation**
Opsin					
Unigene0004368	8.17	rhodopsin [*Penaeus vannamei*]	Unigene0037728	90,886.59	rhodopsin [*Penaeus vannamei*]
Unigene0032821	1.53	rhodopsin-like [*Penaeus vannamei*]	Unigene0025543	63.29	LWS opsin [*Macrobrachium nipponense*]
Unigene0042144	40.68	rhodopsin-like [*Penaeus vannamei*]	Unigene0033598	180.53	LWS opsin [*Macrobrachium nipponense*]
Unigene0027123	1.70	LWS opsin [*Macrobrachium nipponense*]	Unigene0034802	15,756.87	LWS opsin [*Macrobrachium nipponense*]
Unigene0036486	2.92	opsin protein [*Leptuca pugilator*]	Unigene0009342	15.00	LWS opsin [*Macrobrachium nipponense*]
			Unigene0028409	20.80	opsin protein [*Leptuca pugilator*]
			Unigene0032948	1417.97	opsin protein [*Leptuca pugilator*]
			Unigene0023137	30.24	opsin protein [*Leptuca pugilator*]
			Unigene0023206	5.03	opsin [*Penaeus vannamei*]
			Unigene0030878	62.38	opsin 1 [*Gelasimus vomeris*]
			Unigene0027784	10.57	UV2 opsin [*Penaeus vannamei*]
			Unigene0032158	375.03	UV2 opsin [*Penaeus vannamei*]
			Unigene0032059	158.62	opsin, UVS-like [*Penaeus vannamei*]
Gq					
Unigene0018293	1.70	$G\alpha_q$ [*Litopenaeus vannamei*]	Unigene0029827	306.06	$G\alpha_q$ [*Litopenaeus vannamei*]
Unigene0018292	6.81	$G\alpha_q$ [*Panulirus argus*]	Unigene0019099	1.37	Gα [*Anopheles gambiae*]
Unigene0005837	20.00	Gγ [*Megachile rotundata*]	Unigene0035586	88.09	Gγ [*Megachile rotundata*]
			Unigene0036996	147.32	Gβ [*Hyalella azteca*]
PLC					
Unigene0047519	7.07	1-phosphatidylinositol 4,5-bisphosphate phosphodiesterase classes I and II isoform X2 [*Cimex lectularius*]	Unigene0032290	3.50	1-phosphatidylinositol 4,5-bisphosphate phosphodiesterase classes I and II isoform X1 [*Cimex lectularius*]
			Unigene0007465	38.34	phospholipid phospholipase C beta isoform [*Homarus americanus*]
PKC					
Unigene0035146	3.53	PKC, brain isozyme [*Trachymyrmex cornetzi*]	Unigene0037047	12.51	PKC, brain isozyme [*Cimex lectularius*]
TRP					
Unigene0031956	1.28	TRP protein-like [*Plutella xylostella*]	Unigene0041701	4.31	TRP protein-like [*Tribolium castaneum*]
Unigene0008099	1.87	TRP protein-like [*Hyalella azteca*]	Unigene0025995	4.03	TRP protein-like [*Hyalella azteca*]
			Unigene0036355	138.36	TRP protein-like [*Hyalella azteca*]
			Unigene0025996	3.12	TRP protein [*Orchesella cincta*]
			Unigene0037466	63.95	TRP channel [*Danaus plexippus*]
TRPL					
Unigene0002671	2.20	TRPL protein [*Hyalella azteca*]	Unigene0036670	1807.23	TRPL protein [*Hyalella azteca*]
Unigene0009926	1.04	TRPL protein [*Hyalella azteca*]			
CaM					
Unigene0041980	2.74	calmodulin-alpha isoform [*Papilio machaon*]	Unigene0046282	1.20	calmodulin-beta-like isoform [*Aethina tumida*]
			Unigene0028022	1207.07	calmodulin [*Trichinella pseudospiralis*]
			Unigene0034208	21.68	calmodulin-like protein [*Zootermopsis nevadensis*]
NINAC					
Unigene0013894	1.68	myosin-IIIb-like [*Hyalella azteca*]	Unigene0036698	109.85	myosin-IIIb-like [*Hyalella azteca*]
			Unigene0036679	46.20	myosin-IIIb-like [*Orussus abietinus*]
			Unigene0036678	79.34	NINAC-like isoform [*Hyalella azteca*]

Table 2. *Cont.*

Alvinocaris longirostris			*Palaemon carinicauda*		
Gene ID	**RPKM**	**Annotation**	**GeneID**	**RPKM**	**Annotation**
Arrestin					
Unigene0037454	1.79	arrestin homolog [*Hyalella azteca*]	Unigene0031031	135.94	arrestin homolog [*Hyalella azteca*]
			Unigene0031684	117.09	arrestin homolog [*Hyalella azteca*]
			Unigene0036855	33074.95	arrestin homolog [*Hyalella azteca*]
			Unigene0030229	6832.96	arrestin homolog [*Hyalella azteca*]
			Unigene0029989	609.90	arrestin [*Orchesella cincta*]
DAGL					
Unigene0045000	2.47	DAGL alpha-like [*Hyalella azteca*]			
Actin					
Unigene0050853	29.43	actin [*Eulimnogammarus vittatus*]	Unigene0038263	91.80	actin [*Eulimnogammarus cyaneus*]
Unigene0014222	1.0	actin [*Chilodonella uncinata*]	Unigene0034159	1824.31	beta-actin [*Macrobrachium nipponense*]
Unigene0002593	8.28	actin [*Portunus trituberculatus*]	Unigene0035399	2.07	actin 1 [*Procambarus clarkii*]
Unigene0046083	14.64	actin 1 [*Procambarus clarkii*]	Unigene0038246	9.52	actin-2 [*Penaeus vannamei*]
Unigene0046852	2532.89	beta-actin [*Penaeus monodon*]	Unigene0035402	13.00	actin 1 [*Penaeus vannamei*]
Unigene0039765	128.24	actin 6 [*Pandalus platyceros*]	Unigene0035632	15.64	actin 6 [*Pandalus platyceros*]
Unigene0014452	1.69	actin [*Armadillidium vulgare*]	Unigene0038264	1.67	actin [*Penaeus vannamei*]
Unigene0012144	686.58	skeletal muscle actin 6 [*Rimicaris exoculata*]	Unigene0035395	5.76	skeletal muscle actin 6 [*Rimicaris exoculata*]
Unigene0034554	16.89	actin-like [*Penaeus vannamei*]	Unigene0038262	39.92	skeletal muscle actin 6 [*Palaemon varians*]
Unigene0009093	12.08	actin-2 [*Penaeus vannamei*]	Unigene0034152	80.94	actin-like [*Penaeus vannamei*]
			Unigene0038252	111.22	skeletal muscle actin 8 [*Homarus americanus*]
			Unigene0034150	65.39	skeletal muscle alpha actin [*Pandalus platyceros*]
			Unigene0035634	25.35	actin 2 [*Penaeus vannamei*]
INAD PDZ					
Unigene0046429	4.50	multiple PDZ domain protein [*Portunus trituberculatus*]	Unigene0011764	1.83	PDZ domain-containing protein 2 [*Portunus trituberculatus*]
Unigene0000247	1.57	multiple PDZ domain protein-like [*Zootermopsis nevadensis*]	Unigene0020200	1.52	PDZ domain-containing protein 2 [*Penaeus vannamei*]
Unigene0042843	3.33	PDZ domain-containing protein 2 [*Penaeus vannamei*]	Unigene0034891	38.85	multiple PDZ domain protein-like isoform X5 [*Penaeus vannamei*]
			Unigene0026310	3.19	PDZ domain-containing protein 2 [*Penaeus vannamei*]

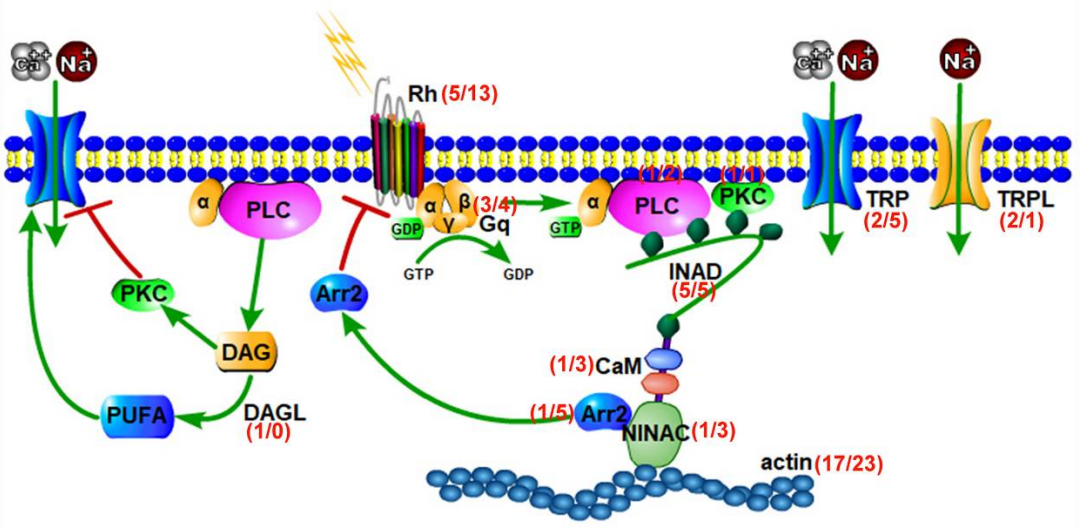

Figure 4. Opsin-mediated phototransduction pathway. The number of corresponding genes is listed in the red bracket (*Alvinocaris longirostris*/*Palaemon carinicauda*).

The topology of the phylogenetic tree of opsins demonstrates the monophyletic clades of LWS opsins and SWS/UVS opsins, respectively, while the insect MWS clade is the sister group to the LWS clade (Figure 5), and the sequenced MWS opsins in crustacean fall outside of the main arthropod LWS clade and insect MWS. Based on the phylogenetic analysis,

four candidate LWS opsins and one MWS opsin in *A. longirostris* eye transcriptome were identified, while there were five putative LWS opsins, five MWS opsins and another three SWS/UVS opsins in *P. carinicauda* transcriptome (Figure 5). It is noteworthy that SWS/UVS opsins were absent in *A. longirostris*, and fewer MWS opsins were discovered in this deep-sea shrimp. In comparison, putative LWS opsins showed relatively high expression level in *A. longirostris* and *P. carinicauda*, respectively. Amino acid sequence alignments were then further performed on the LWS opsins from deep-sea and shallow-water decapods (Table S1). It was revealed that conservative domains and sites were present in all opsins (Figure S3), including the seven-transmembrane (TM), the critical chromophore attachment site at K296, the important rhodopsin-class GRCR domain (E)DRY, glutamate counterion candidate E181 and two cysterine residues (C110, C187) potentially involved in the disulfide bond [55]. It indicates that the key opsins in these deep-sea crustaceans may conserve their signal transduction function.

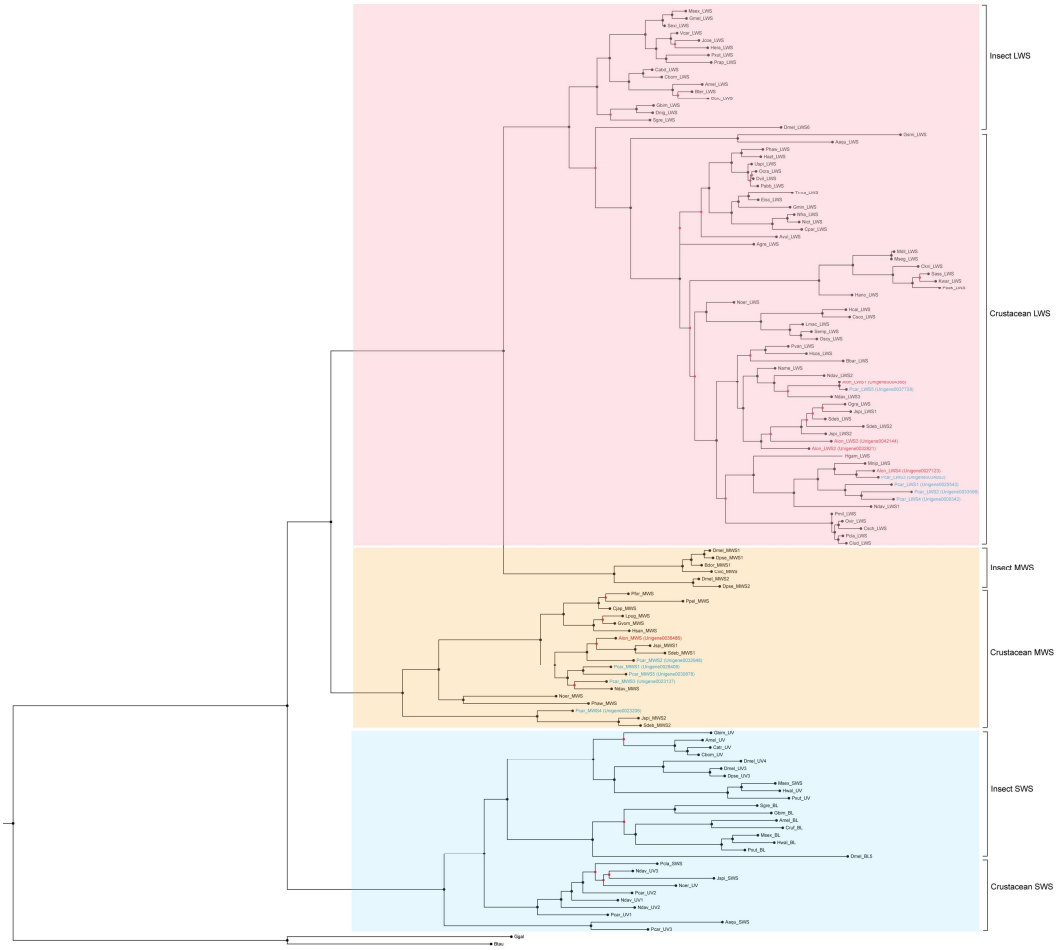

Figure 5. Maximum-likelihood phylogeny of opsin visual proteins in representative arthropod species. The tree is constructed based on the amino acid sequences. *Bos taurus* rhodopsin and *Gallus gallus* pinopsin sequences serve as out-group. Most bootstrap support is significant, and the low support is indicated by red circles (SH-aLRT < 80, or UFBoot < 95, and aBayes < 0.95). LWS (long-wavelength-sensitive) opsins, MWS (middle-wavelength-sensitive) opsins and SWS/UVS (short-wavelength/UV-sensitive) opsins are located in areas with different color. Opsins in *Alvinocaris longirostris* and *Palaemon carinicauda* are marked with red and yellow, respectively. The detailed information of sequences used to construct phylogenetic tree is described in Table S1.

4. Discussion

In the deep-sea aphotic zone, many crustaceans and fish have reduced eyes or lack eyes completely. Most existing studies have focused on the morphological and physiological characters of deep-sea animal eyes (reviewed in [7]). Our study based on the comparative transcriptomes of deep-sea *A. longirostris* and shallow-water *P. carinicauda* eyes provides basic gene resources to elucidate the molecular mechanism of eye development and phototransduction of alvinocaridid shrimps in deep-sea chemosynthetic ecosystems.

Previous studies have improved our understanding of retinal determination network that influence eye development. In a limited capacity, researchers have focused on the compound eyes of insects such as *Drosophila*, and there are few molecular studies on the development of compound eyes of crustaceans. It has been discovered that loss of *ey* is linked to the headless phenotype in *Drosophila*, while *toy* acts upstream of *ey* and activates its expression [56–60]. In this study, the key genes in retinal determination network have been identified in the deep-sea and shallow-water shrimps, and two 'master regulator' *Pax6* paralogs, *ey* and *toy*, are present in the two species. However, the gene expression level of *ey* and *toy* is low in both shrimp species, probably due to the fact that *ey* and *toy* mainly act early during eye development in invertebrates [61]. It has also been observed that the eyes of alvinocaridid shrimp and the hydrothermal vent crab *Bythograea thermidron* present a clear switch between the larvae and adults, from an imaging retina to the non-imaging retina: the zoeal eye is similar to those of other surface-dwelling decapod larvae [62–64]. Therefore, based on the identification of important genes involved in retinal determination network in the two adult shrimps, it is hypothesized that the molecular mechanism of eye development at the embryo–larvae stages in deep-sea chemosynthetic *A. longirostris* and shallow-water *P. carinicauda* might be similar, which requires further verification in samples from early developmental stages.

Visual processing begins with photoreceptors that convert photon energy into an electrical signal transmitted to the nervous system. Opsin, G-protein, PLC, TRP and TRPL channels are critical components in phototransduction of invertebrates [65]. The development of genomics and transcriptomics has made comparative studies of visual systems more feasible [66,67]. In this study, visual related expressed genes are less abundant in deep-sea *A. longirostris*, similar to the situation in cave fishes, cave shrimps and other deep-sea crustaceans [32–34,45,46]. A different number of *opsin* genes between *A. longirostris* and *P. carinicauda* have been identified, which might correlate with the life-history, habitat and the ecological niches the animals occupy [68,69]. By constructing the phylogenetic tree of representative arthropod opsins, the evolutionary placement of opsins in *A. longirostris* and *P. carinicauda* is determined and the spectral sensitivity of the opsins in the two shrimps is inferred, although it requires experimental quantification. The light emitted by the hot hydrothermal plume is usually in the form of long wavelength radiation (>700 nm), and temporally variable light is observed in the 400–600 nm region of the spectrum [70]. Moreover, the vast majority of bioluminescence lies about 450–510 nm [71–73]. In this study, more transcripts of putative LWS (>490 nm) *opsins* are expressed in both species, which is consistent with the results of other studies on the photoreceptors of crustaceans [28,74–76]. The conserved sites and structures of the LWS opsins have been found between deep-sea and shallow-water decapods, indicating that these opsins in deep-sea crustaceans may also conserve their spectral absorption and signal transduction function. Moreover, a putative MWS (400–490 nm) *opsin* is also detected. Therefore, we interpret that the degenerate eyes of *A. longirostris* might retain the function of detecting low-level illumination in the deep-sea chemosynthetic environments. However, due to the absence of SWS light in the deep sea [77,78], no SWS/UVS (<400 nm) opsin has been discovered expressed in eyes of deep-sea *A. longirostris* adults. In general, *opsins* in deep-sea *A. longirostris* show reduced expression levels (the highest RPKM 40.68) compared to those of shallow-water *P. carinicauda* (the highest RPKM 90,886.59), which has also been found in the retinas of cave crustacean, cavefish and the hydrothermal vent crab *Austinograea alayseae* [30,31,79], as well as a reduction in their total absorbance spectra [35]. In addition, studies found

that TRP and TRPL are potently activated by polyunsaturated fatty acids (PUFAs), which could be released from DAG by DAGL [80,81]. The gene *DAGL* has only been found in the deep-sea *A. longirostris*, which may indicate that there are additional messengers that could result in the opening of the TRP and TRPL channels in this shrimp species. The divergence in the number and type of different phototransduction related genes, especially *opsins*, could be a strategy to adapt to specific spectral ranges in deep-sea chemosynthetic ecosystems. Although the absence of particular types of opsins does not indicate absence from the genome, we can at least estimate the number of transcripts represented in the transcriptome of each species as a baseline for further studies.

5. Conclusions

In this study, the eye transcriptomes of deep-sea *A. longirostris* and shallow-water *P. carinicauda* were compared. Key transcription factor genes involved in retinal development were all recovered in both species. It is hypothesized that eye development processes at the larval stages of the two shrimps might be similar and the eyes of *A. longirostris* degenerate during the late developmental stage, which requires the gene expression data of larval samples for verification. In comparison with the shallow-water shrimps, the number and expression level of genes involved in phototransduction pathway were significantly reduced in *A. longirostris*. The lack of SWS *opsin* and the low amount of MWS *opsin* likely resulted from the restricted spectral range of the deep-sea chemosynthetic environment. The conserved sites and structures of LWS opsins between deep-sea and shallow-water shrimps suggested the conserved function of the genes. These may correlate with the life-history and habitat of *A. longirostris*. The complete list of visual-related genes should be pursued by whole genome sequencing as this study is intended to supply baseline transcript information for further investigation.

Supplementary Materials: The following supporting information can be downloaded at: https://www.mdpi.com/article/10.3390/d14080653/s1, Figure S1: The regulated network of eye development related transcription factors eyeless (ey), twin of eyeless (toy), sine oculis (so), eyes absent (eya), dachshund (dac), hedgehog (hh), and decapentaplegic (dpp) (revised according to [16]); Figure S2: GO function classification of annotated genes in the transcriptomes of *Alvinocaris longirostris* and *Palaemon carinicauda*; Figure S3: Sequence alignment of LWS (long-wavelength sensitive) opsins from deep-sea species and shallow-water decapod species. Conserved sites and structures of the opsins are analyzed and marked with *Bos taurus* rhodopsin sequence as a model (accession number: NM 001014890.2). Black boxes encircle the transmembrane alpha-helices 1–7 of opsins. C110 and C187 are potentially involved in a disulfide bond. The DRY-type tripeptide motif (D134, R135, Y136) is marked by asterisks. E181 is the glutamate counterion position. K296 is involved in the formation of Schiff base linkage; Table S1: Arthropod opsin sequences used to construct phylogenetic tree; Table S2: Pax sequences used to construct phylogenetic tree; Table S3: Eye development related transcription factors from eye transcriptomes of *Alvinocaris longirostris* and *Palaemon carinicauda*. Paired box protein 6 (Pax6), eyeless (ey), twin of eyeless (toy), sine oculis (so), eyes absent (eya), dachshund (dac), hedgehog (hh), and decapentaplegic (dpp).

Author Contributions: Conceptualization, M.H. and Z.S.; formal analysis, M.H., Q.X. and J.C.; writing—original draft preparation, M.H. and Q.X.; writing—review and editing, M.H., J.C. and Z.S.; funding acquisition, M.H., J.C. and Z.S. All authors have read and agreed to the published version of the manuscript.

Funding: This research was funded by the Key Deployment Project of Centre for Ocean Mega-Research of Science, Chinese Academy of Sciences (CAS), grant number COMS2019Q042; the National Natural Science Foundation of China, grant number 31872215; the National Science Foundation for Distinguished Young Scholars, grant number 42025603; and the Strategic Priority Research Program of CAS, grant number XDB42000000. The APC was funded by the National Natural Science Foundation of China, grant number 31872215.

Institutional Review Board Statement: Not applicable.

Informed Consent Statement: Not applicable.

Data Availability Statement: The Illumina data for *P. carinicauda* and *A. longirostris* eye samples have been deposited into the Sequence Read Archive (SRA) database (http://www.ncbi.nlm.nih.gov/Traces/sra/; accessed on 22 March 2020) with the accession number PRJNA597836 and PRJNA548620, respectively.

Acknowledgments: The samples were collected by RV KEXUE. The authors wish to thank the crews for their help during the collection of the samples.

Conflicts of Interest: The authors declare no conflict of interest.

References

1. Van Dover, C.L. *The Ecology of Deep-Sea Hydrothermal Vents*; Princeton University Press: Princeton, NJ, USA, 2000.
2. Levin, L.A. Ecology of cold seep sediments: Interactions of fauna with flow, chemistry and microbes. *Oceanogr. Mar. Biol.* **2005**, *43*, 11–56.
3. White, S.N.; Chave, A.D.; Reynolds, G.T.; Gaidos, E.J.; Tyson, J.A.; Van Dover, C.L. Variations in ambient light emission from black smokers and flange pools on the Juan De Fuca Ridge. *Geophys. Res. Lett.* **2000**, *27*, 1151–1154. [CrossRef]
4. Reynolds, G.T.; Lutz, R.A. Sources of light in the deep ocean. *Rev. Geophys.* **2001**, *39*, 123–136. [CrossRef]
5. Widder, E.A. Bioluminescence in the ocean: Origins of biological, chemical, and ecological diversity. *Science* **2010**, *328*, 704–708. [CrossRef] [PubMed]
6. Johnsen, S.; Frank, T.M.; Haddock, S.H.D.; Widder, E.A.; Messing, C.G. Light and vision in the deep-sea benthos: I. Bioluminescence at 500–1000 m depth in the Bahamian Islands. *J. Exp. Biol.* **2012**, *215*, 3335–3343. [CrossRef] [PubMed]
7. Warrant, E.J.; Locket, N.A. Vision in the deep sea. *Biol. Rev.* **2004**, *79*, 671–712. [CrossRef]
8. Hiller-Adams, P.; Case, J.F. Optical parameters of euphausiid eyes as a function of habitat depth. *J. Comp. Physiol. A* **1984**, *154*, 307–318. [CrossRef]
9. Hiller-Adams, P.; Case, J.F. Eye size of pelagic crustaceans as a function of habitat depth and possession of photophores. *Vision Res.* **1988**, *28*, 667–680. [CrossRef]
10. Wharton, D.N.; Jinks, R.N.; Herzog, E.D.; Battelle, B.A.; Kass, L.; Renninger, G.H.; Chamberlain, S.C. Morphology of the eye of the hydrothermal vent shrimp, *Alvinocaris markensis*. *J. Mar. Biol. Assoc. UK* **1997**, *77*, 1097–1108. [CrossRef]
11. Elofsson, R.; Hallberg, E. Compound eyes of some deep-sea and Fiord Mysid crustaceans. *Acta Zool.* **1977**, *58*, 169–177. [CrossRef]
12. Chamberlain, S.C.; Meyer-Rochow, V.B.; Dossert, W.P. Morphology of the eye of the giant deep-sea isopod *Bathynomus giganteus*. *J. Morphol.* **1986**, *189*, 145–156. [CrossRef]
13. Meyer-Rochow, V.B.; Nilsson, H.L. Compound eyes in polar regions, caves and the deep-sea. In *Atlas of Arthropod Sensory Receptors*; Eguchi, E., Tominaga, Y., Eds.; Springer: Berlin, Germany; Tokyo, Japan; New York, NY, USA, 1998; pp. 125–142.
14. Van Dover, C.L.; Szuts, E.Z.; Chamberlain, S.C.; Cann, J.R. A novel eye in "eyeless" shrimp from hydrothermal vents of the Mid-Atlantic Ridge. *Nature* **1989**, *337*, 458–460. [CrossRef]
15. Land, M.F. Vision: What is a naked retina good for? *Nature* **2002**, *420*, 30–31. [CrossRef]
16. Tsachaki, M.; Sprecher, S.G. Genetic and developmental mechanisms underlying the formation of the *Drosophila* compound eye. *Dev. Dynam.* **2012**, *241*, 40–56. [CrossRef]
17. Jacobsson, L.; Kronhamn, J.; Rasmuson-Lestander, A. The *Drosophila* Pax6 paralogs have different functions in head development but can partially substitute for each other. *Mol. Genet. Genom.* **2009**, *282*, 217–231. [CrossRef]
18. Pignoni, F.; Hu, B.; Zavitz, K.H.; Xiao, J.; Garrity, P.A.; Zipursky, L. The eye-specification proteins So and Eya form a complex and regulate multiple steps in *Drosophila* eye development. *Cell* **1997**, *91*, 881–891. [CrossRef]
19. Pappu, K.S.; Chen, R.; Middlebrooks, B.W.; Woo, C.; Heberlein, U.; Mardon, G. Mechanism of hedgehog signaling during *Drosophila* eye development. *Development* **2003**, *130*, 3053–3062. [CrossRef] [PubMed]
20. Curtiss, J.; Mlodzik, M. Morphogenetic furrow initiation and progression during eye development in *Drosophila*: The roles of *decapentaplegic*, *hedgehog* and *eyes absent*. *Development* **2000**, *127*, 1325–1336. [CrossRef]
21. Yang, X.; ZarinKamar, N.; Bao, R.; Friedrich, M. Probing the *Drosophila* retinal determination gene network in *Tribolium* (I): The early retinal genes *dachshund*, *eyes absent* and *sine oculis*. *Dev. Biol.* **2009**, *333*, 202–214. [CrossRef]
22. Jeffery, W.R. Adaptive evolution of eye degeneration in the Mexican blind cavefish. *J. Hered.* **2005**, *96*, 185–196. [CrossRef]
23. Jeffery, W.R. Evolution and development in the cavefish *Astyanax*. *Curr. Top. Dev. Biol.* **2009**, *86*, 191–221. [PubMed]
24. Meng, F.; Braasch, I.; Phillips, J.B.; Lin, X.; Titus, T.; Zhang, C.; Postlethwait, J.H. Evolution of the eye transcriptome under constant darkness in *Sinocyclocheilus* cavefish. *Mol. Biol. Evol.* **2013**, *30*, 1527–1543. [CrossRef] [PubMed]
25. Carroll, S.B. Evolution at two levels: On genes and form. *PLoS Biol.* **2005**, *3*, e245. [CrossRef]
26. Hardie, R.C. Phototransduction in *Drosophila melanogaster*. *J. Exp. Biol.* **2001**, *204*, 3403–3409. [CrossRef] [PubMed]
27. Porter, M.L.; Blasic, J.R.; Bok, M.J.; Cameron, E.G.; Pringle, T.; Cronin, T.W.; Robinson, P.R. Shedding new light on opsin evolution. *Proc. R. Soc. B* **2012**, *279*, 3–14. [CrossRef] [PubMed]
28. Rajkumar, P.; Rollmann, S.M.; Cook, T.A.; Layne, J.E. Molecular evidence for color discrimination in the Atlantic sand fiddler crab, *Uca pugilator*. *J. Exp. Biol.* **2010**, *213*, 4240–4248. [CrossRef] [PubMed]
29. Cronin, T.W.; Hariyama, T. Spectral sensitivity in crustacean eyes. In *The Crustacean Nervous System*; Wiese, K., Ed.; Springer: Berlin/Heidelberg, Germany, 2002; pp. 499–511.

30. Langecker, T.G.; Schmale, H.; Wilkens, H. Transcription of the *opsin* gene in degenerate eyes of cave-dwelling *Astyanax fasciatus* (Teleostei, Characidae) and of its conspecific epigean ancestor during early ontogeny. *Cell Tissue Res.* **1993**, *273*, 183–192. [CrossRef]
31. Carlini, D.B.; Satish, S.; Fong, D.W. Parallel reduction in expression, but no loss of functional constraint, in two opsin paralogs within cave populations of *Gammarus minus* (Crustacea: Amphipoda). *BMC Evol. Biol.* **2013**, *13*, 89. [CrossRef] [PubMed]
32. Gross, J.B.; Furterer, A.; Carlson, B.M.; Stahl, B.A. An integrated transcriptome-wide analysis of cave and surface dwelling *Astyanax mexicanus*. *PLoS ONE* **2013**, *8*, e55659. [CrossRef]
33. Hinaux, H.; Poulain, J.; da Silva, C.; Noirot, C.; Jeffery, W.R.; Casane, D.; Retaux, S. *De novo* sequencing of *Astyanax mexicanus* surface fish and pachon cavefish transcriptomes reveals enrichment of mutations in cavefish putative eye genes. *PLoS ONE* **2013**, *8*, e53553. [CrossRef]
34. Stern, D.B.; Crandall, K.A. Phototransduction gene expression and evolution in cave and surface crayfishes. *Integr. Comp. Biol.* **2018**, *58*, 398–410. [CrossRef]
35. Mejía-Ortíz, L.M.; Hartnoll, R.G. Modifications of eye structure and integumental pigment in two cave crayfish. *J. Crustacean Biol.* **2005**, *25*, 480–487. [CrossRef]
36. Komai, T.; Segonzac, M. A revision of the genus *Alvinocaris* Williams and Chace (Crustacea: Decapoda: Caridea: Alvinocarididae), with descriptions of a new genus and a new species of *Alvinocaris*. *J. Nat. Hist.* **2005**, *39*, 1111–1175. [CrossRef]
37. Sun, S.; Sha, Z.; Wang, Y. Phylogenetic position of Alvinocarididae (Crustacea: Decapoda: Caridea): New insights into the origin and evolutionary history of the hydrothermal vent alvinocarid shrimps. *Deep-Sea Res. Part I* **2018**, *141*, 93–105. [CrossRef]
38. Xin, Q.; Hui, M.; Sha, Z. Eyes of differing colors in *Alvinocaris longirostris* from deep-sea chemosynthetic ecosystems: Genetic and molecular evidence of its formation mechanism. *J. Oceanol. Limnol.* **2021**, *39*, 282–296. [CrossRef]
39. Grabherr, M.G.; Haas, B.J.; Yassour, M.; Levin, J.Z.; Thompson, D.A.; Amit, I.; Adiconis, X.; Fan, L.; Raychowdhury, R.; Zeng, Q.; et al. Full-length transcriptome assembly from RNA-Seq data without a reference genome. *Nat. Biotechnol.* **2011**, *29*, 644–652. [CrossRef]
40. Manni, M.; Berkeley, M.R.; Seppey, M.; Simão, F.A.; Zdobnov, E.M. BUSCO update: Novel and streamlined workflows along with broader and deeper phylogenetic coverage for scoring of eukaryotic, prokaryotic, and viral genomes. *Mol. Biol. Evol.* **2021**, *38*, 4647–4654. [CrossRef] [PubMed]
41. Manni, M.; Berkeley, M.R.; Seppey, M.; Zdobnov, E.M. BUSCO: Assessing genomic data quality and beyond. *Curr. Protoc.* **2021**, *1*, e323. [CrossRef]
42. Conesa, A.; Gotz, S.; Garcia-Gomez, J.M.; Terol, J.; Talon, M.; Robles, M. Blast2GO: A universal tool for annotation, visualization and analysis in functional genomics research. *Bioinformatics* **2005**, *21*, 3674–3676. [CrossRef] [PubMed]
43. Ye, J. WEGO: A web tool for plotting GO annotations. *Nucleic Acids Res.* **2006**, *34*, W293–W297. [CrossRef] [PubMed]
44. Mortazavi, A.; William, B.A.; Mccue, K.; Schaeffer, L.; Wold, B. Mapping and quantifying mammalian transcriptomes by RNA-Seq. *Nat. Methods* **2008**, *5*, 621–628. [CrossRef]
45. Bracken-Grissom, H.D.; DeLeo, D.M.; Porter, M.L.; Iwanicki, T.; Sickles, J.; Frank, T.M. Light organ photosensitivity in deep-sea shrimp may suggest a novel role in counterillumination. *Sci. Rep.* **2020**, *10*, 4485. [CrossRef]
46. DeLeo, D.M.; Bracken-Grissom, H.D. Illuminating the impact of diel vertical migration on visual gene expression in deep-sea shrimp. *Mol. Ecol.* **2020**, *29*, 3494–3510. [CrossRef]
47. Katoh, K.; Toh, H. Recent developments in the MAFFT multiple sequence alignment program. *Brief. Bioinform.* **2008**, *9*, 286–298. [CrossRef]
48. Shigehiro, K.; Zmasek, C.M.; Osamu, N.; Kazutaka, K. aLeaves facilitates on-demand exploration of metazoan gene family trees on MAFFT sequence alignment server with enhanced interactivity. *Nucleic Acids Res.* **2013**, *41*, W22–W28.
49. Nguyen, L.T.; Schmidt, H.A.; von Haeseler, A.; Minh, B.Q. IQ-TREE: A fast and effective stochastic algorithm for estimating maximum likelihood phylogenies. *Mol. Biol. Evol.* **2015**, *32*, 268–274. [CrossRef]
50. Kalyaanamoorthy, S.; Minh, B.Q.; Wong, T.K.F.; von Haeseler, A.; Jermiin, L.S. ModelFinder: Fast model selection for accurate phylogenetic estimates. *Nat. Methods* **2017**, *14*, 587–589. [CrossRef] [PubMed]
51. Hoang, D.T.; Chernomor, O.; von Haeseler, A.; Minh, B.Q.; Vinh, L.S. UFBoot2: Improving the ultrafast bootstrap approximation. *Mol. Biol. Evol.* **2018**, *35*, 518–522. [CrossRef]
52. Guindon, S.; Dufayard, J.F.; Lefort, V.; Anisimova, M.; Hordijk Wim Gascuel, O. New algorithms and methods to estimate maximum-likelihood phylogenies: Assessing the performance of PhyML 3.0. *Syst. Biol.* **2010**, *59*, 307–321. [CrossRef] [PubMed]
53. Anisimova, M.; Gil, M.; Dufayard, J.F.; Dessimoz, C.; Gascuel, O. Survey of branch support methods demonstrates accuracy, power, and robustness of fast likelihood-based approximation schemes. *Syst. Biol.* **2011**, *60*, 685–699. [CrossRef] [PubMed]
54. Hou, Y.N.; Li, S.; Luan, Y.X. Pax6 in Collembola: Adaptive evolution of eye regression. *Sci. Rep.* **2016**, *6*, 20800. [CrossRef]
55. Terakita, A.; Koyanagi, M.; Tsukamoto, H.; Yamashita, T.; Miyata, T.; Shichida, Y. Counterion displacement in the molecular evolution of the rhodopsin family. *Nat. Struct. Mol. Biol.* **2004**, *11*, 284–289. [CrossRef] [PubMed]
56. Glaser, T.; Walton, D.S.; Maas, R.L. Genomic structure, evolutionary conservation and aniridia mutations in the human *PAX6* gene. *Nat. Genet.* **1992**, *2*, 232–239. [CrossRef]
57. Jordan, T.; Hanson, I.; Zaletayev, D.; Hodgson, S.; Prosser, J.; Seawright, A.; Hastie, N.; van Heyningen, V. The human *PAX6* gene is mutated in two patients with aniridia. *Nat. Genet.* **1992**, *1*, 328–332. [CrossRef]
58. Quiring, R.; Walldorf, U.; Kloter, U.; Gehring, W.J. Homology of the *eyeless* gene of *Drosophila* to the *Small eye* gene in mice and Aniridia in humans. *Science* **1994**, *265*, 785–789. [CrossRef]

59. Kronhamn, J.; Frei, E.; Daube, M.; Jiao, R.; Rasmuson-Lestander, A. Headless flies produced by mutations in the paralogous *Pax6* genes eyeless and twin of eyeless. *Development* **2002**, *129*, 1015–1026. [CrossRef]
60. Czerny, T.; Halder, G.; Kloter, U.; Souabni, A.; Gehring, W.J.; Busslinger, M. Twin of eyeless, a second *Pax-6* gene of *Drosophila*, acts upstream of eyeless in the control of eye development. *Mol. Cell* **1999**, *3*, 297–307. [CrossRef]
61. Punzo, C.; Seimiya, M.; Flister, S.; Gehring, W.J.; Plaza, S. Differential interactions of eyeless and twin of eyeless with the sine oculis enhancer. *Development* **2002**, *129*, 625–634. [CrossRef]
62. Gaten, E.; Herring, P.J.; Shelton, P.M.J.; Johnson, M.L. The development and evolution of the eyes of vent shrimps (Decapoda: Bresiliidae). *Cah. Biol. Mar.* **1998**, *39*, 287–290.
63. Gaten, E.; Herring, P.J.; Shelton, P.M.J.; Johnson, M.L. Comparative morphology of the eyes of postlarval bresiliid shrimps from the region of hydrothermal vents. *Biol. Bull.* **1998**, *194*, 267–280. [CrossRef]
64. Jinks, R.N.; Markley, T.L.; Taylor, E.E.; Perovich, G.; Dittel, A.I.; Epifanio, C.E.; Cronin, T.W. Adaptive visual metamorphosis in a deep-sea hydrothermal vent crab. *Nature* **2002**, *420*, 68–70. [CrossRef] [PubMed]
65. Hardie, R.C.; Postma, M. Phototransduction in microvillar photoreceptors of *Drosophila* and other invertebrates. In *The Senses: A Comprehensive Reference*; Masland, R.H., Albright, T.D., Eds.; Elsevier Inc.: Amsterdam, The Netherlands, 2008; Volume 1, pp. 77–130.
66. Petrash, J.M.; Ruzycki, P.A.; Zablocki, G.J. Visionary genomics. *Hum. Genom.* **2011**, *5*, 519–521. [CrossRef] [PubMed]
67. Porter, M.L.; Speiser, D.I.; Zaharoff, A.K.; Caldwell, R.L.; Cronin, T.W.; Oakley, T.H. The evolution of complexity in the visual systems of stomatopods: Insights from transcriptomics. *Integr. Comp. Biol.* **2013**, *53*, 39–49. [CrossRef]
68. Marshall, J.; Carleton, K.L.; Cronin, T. Colour vision in marine organisms. *Curr. Opin. Neurobiol.* **2015**, *34*, 86–94. [CrossRef]
69. Stieb, S.M.; Cortesi, F.; Sueess, L.; Carleton, K.L.; Salzburger, W.; Marshall, N.J. Why UV vision and red vision are important for damselfish (Pomacentridae): Structural and expression variation in *opsin* genes. *Mol. Ecol.* **2017**, *26*, 1323–1342. [CrossRef] [PubMed]
70. White, S.N.; Chave, A.D. Investigations of ambient light emission at deep-sea hydrothermal vents. *J. Geophys. Res.* **2002**, *107*, 2001. [CrossRef]
71. Herring, P.J. The spectral characteristics of luminous marine organisms. *Proc. R. Soc. Lond. B* **1983**, *220*, 183–217.
72. Widder, E.A.; Latz, M.I.; Case, J.F. Marine bioluminescence spectra measured with an optical multichannel detection system. *Biol. Bull.* **1983**, *165*, 791–810. [CrossRef]
73. Haddock, S.H.D.; Case, J.F. Bioluminescence spectra of shallow and deep-sea gelatinous zooplankton: Ctenophores, medusae, and siphonophores. *Mar. Biol.* **1999**, *133*, 571–582. [CrossRef]
74. Oakley, T.H.; Huber, D.R. Differential expression of duplicated *opsin* genes in two eye types of ostracod crustaceans. *J. Mol. Evol.* **2004**, *59*, 239–249. [CrossRef]
75. Porter, M.L.; Cronin, T.W.; McClellan, D.A.; Crandall, K.A. Molecular characterization of crustacean visual pigments and the evolution of pancrustacean opsins. *Mol. Biol. Evol.* **2007**, *24*, 253–268. [CrossRef] [PubMed]
76. Porter, M.L.; Bok, M.J.; Robinson, P.R.; Cronin, T.W. Molecular diversity of visual pigments in Stomatopoda (Crustacea). *Visual Neurosci.* **2009**, *26*, 255–265. [CrossRef] [PubMed]
77. Denton, E.J. Light and vision at depths greater than 200 metres. In *The Visual System of Fish*; Douglas, R.H., Djamqoz, M.B.A., Eds.; Chapman & Hall: London, UK, 1990; pp. 127–148.
78. Douglas, R.H.; Hunt, D.M.; Bowmaker, J.K. Spectral sensitivity tuning in the deep-sea. In *Sensory Processing in Aquatic Environments*; Collin, S.P., Marshall, N.J., Eds.; Springer New York Inc.: New York, NY, USA, 2003; pp. 323–342.
79. Hui, M.; Song, C.; Liu, Y.; Li, C.; Cui, Z. Exploring the molecular basis of adaptive evolution in hydrothermal vent crab *Austinograea alayseae* by transcriptome analysis. *PLoS ONE* **2017**, *12*, e0178417. [CrossRef] [PubMed]
80. Leung, H.T.; Tseng-Crank, J.; Kim, E.; Mahapatra, C.; Shino, S.; Zhou, Y.; An, L.; Doerge, R.W.; Pak, W.L. DAG lipase activity is necessary for TRP channel regulation in *Drosophila* photoreceptors. *Neuron* **2008**, *58*, 884–896. [CrossRef]
81. Lev, S.; Katz, B.; Tzarfaty, V.; Minke, B. Signal-dependent hydrolysis of phosphatidylinositol 4,5-bisphosphate without activation of phospholipase C: Implications on gating of *Drosophila* TRPL (transient receptor potential-like) channel. *J. Biol. Chem.* **2012**, *287*, 1436–1447. [CrossRef]